JOURNAL OF CARDIOVASCULAR MAGNETIC RESONANCE®
Vol. 6, No. 1, pp. 33–42, 2004

VIABILITY

# The Partition Coefficient of Gd-DTPA Reflects Maintained Tissue Viability in a Canine Model of Chronic Significant Coronary Stenosis

**Katie S. Lekx,[1,*] Frank S. Prato,[1] Jane Sykes,[1] and Gerald Wisenberg[2]**

[1]Department of Nuclear Medicine, Imaging Program, Lawson Health Research Institute, and [2]Division of Cardiology and The Department of Medical Biophysics, University of Western Ontario, London, Ontario, Canada

## ABSTRACT

*Purpose*. The underlying assumption in delayed enhancement or constant infusion techniques to detect infarcted myocardium is that the partition coefficient (λ) of Gd-DTPA only increases in permanently damaged tissue. This assumption is supported in canine models of stunned and infarcted myocardium but has not been adequately tested in models of chronic, reversibly damaged tissue. *Methods*. A significant coronary stenosis was maintained for 3 (n=9) or 10 (n=4) weeks in a canine model. Myocardial perfusion was assessed using radioactively labeled microspheres, and Doppler flow was used to monitor the effect on flow caused by the stenosis formation. Function and in vivo λ were assessed using magnetic resonance imaging (MRI) and a constant infusion of Gd-DTPA. $^{201}$Tl and $^{111}$In-DTPA were used to assess ex vivo myocardial viability and λ, respectively. *Results*. Baseline Doppler-measured blood flow through the left anterior descending coronary artery was reduced by 72.4±1.6% (SEM) during the stenosis formation. However, shortly after creation of the stenosis and at sacrifice, regional myocardial blood flow at rest was not decreased in the Region at Risk (RAR) despite the persistence of the stenosis. Perfusion reserve in this model, measured using adenosine stress, was significantly reduced. The in vivo λ values in the RAR and remote tissue ranged between 0.32–0.45 mL/g and 0.31–0.42 mL/g, respectively. $^{201}$Tl uptake was maintained in all tissue, confirming the maintenance of tissue viability. Global function was unchanged while regional function was significantly depressed at 10 days but returned to baseline values by

*Correspondence: Katie S. Lekx, Department of Nuclear Medicine, St. Joseph's Health Care, 268 Grosvenor St., London, Ontario N6A 4V2, Canada; Fax: 519-646-6399; E-mail: klekx@lri.sjhc.london.on.ca.



DOI: 10.1081/JCMR-120027803
1097-6647 (Print); 1532-429X (Online)

day 21. *Conclusions*. This study is consistent with the hypothesis that λ is not increased in reversibly dysfunctional myocardium.

*Key Words:* MR imaging; Myocardial viability; Canine model; Coronary artery disease; Significant coronary artery stenosis; Gd-DTPA; Partition Coefficient.

## INTRODUCTION

Coronary artery disease (CAD) remains the largest cause of morbidity and mortality in developed countries (Wijns et al., 1998), and the extent of left ventricular dysfunction is one of the most important prognostic determinants. The extent of functional impairment varies, particularly in postmyocardial infarction patients and those with severe coronary artery disease, and revascularization of the myocardium may result in the recovery of function (Wijns et al., 1998). This improvement in function does not occur, however, if the majority of the functional impairment is secondary to myocardial infarction (by definition irreversible) or extensive fibrosis. Therefore, functional improvement can only occur if there is residual viability in these regions, with minimal fibrosis. Distinguishing different types of reversible injury from irreversible damage is of clinical importance in order to appropriately select patients for revascularization and to aid in determining an individual patient's prognosis.

Previous experiments in our laboratory have investigated infarcted and stunned myocardium using gadolinium diethylenetriaminepetaacetic acid (Gd-DTPA) with magnetic resonance imaging (MRI) (Pereira et al., 2000; Thornhill et al., 2001). In both cases, a constant infusion of Gd-DTPA was used to assess the specificity and sensitivity of differentiating injured (either reversibly or irreversibly) myocardial tissue from normal, healthy myocardial tissue. Pereira et al. (2000) confirmed the sensitivity of the method in their models of both acute and chronic myocardial infarction while Thornhill et al. (2001) confirmed the specificity of this method in a model of stunned myocardium. The determination of distribution volume in different forms of reversibly injured tissue is of interest since some authors (Kim et al., 2000; Pereira et al., 2000; Thornhill et al., 2001) claim that the partition coefficient (λ) is only increased in infarcted tissue, while others (Oshinski et al., 2001; Schwitter et al., 1997) claim that reversibly injured tissue also produces increases in λ and, therefore, the specificity of MRI for determining myocardial viability has been questioned. Our hypothesis was that myocytes subtended by a significantly stenosed coronary artery, but with impaired left ventricular function, would still have the ability to exclude Gd-DTPA and the tissue would not enhance on $T_1$-weighted images. Thus, the partition coefficient of Gd-DTPA would be similar to that found in stunned and normal myocardium. If true, this would further support MRI, with a constant infusion of Gd-DTPA, as both a sensitive and specific method for the determination of tissue viability.

In this study we produced a canine model of significant, perfusion reserve limiting stenosis and confirmed, using measures of viability, function, and regional myocardial blood flow, the presence of reversible myocardial injury and measured the distribution volume of Gd-DTPA in myocardial tissue served by the stenosis.

## METHODS

### Canine Model

After several preliminary experiments, we determined that a reduction of blood flow through the left anterior descending (LAD) coronary artery, measured using Doppler ultrasound, to 20–30% of baseline was the maximum degree of flow reduction possible before permanent myocardial damage (infarction) occurred. The change in blood flow was created using a circumferential stenosing device and measured using a Doppler flow probe (Transonic Systems Inc., Ithaca, NY) placed around the LAD artery immediately proximal to the stenosis. Two different approaches were used to create a ''permanent'' coronary artery stenosis. In four dogs, a balloon occluder was used that allowed small incremental changes in blood flow until the desired degree of stenosis was achieved. However, since balloon occluders can deflate over time, we used a second method in nine dogs once we had determined the degree of stenosis required. The second stenosing device was a self-locking, electrical tie (approximately 5mm in width) surrounded by a hollow plastic cylinder or tubing to cushion the vessel. Selective coronary angiography was performed either following surgery or prior to sacrifice to validate the patency of the stenosed artery and confirm methodology. Absolute regional myocardial blood flow was assessed at various points throughout the experiment using differently labeled radioactive microspheres. The MR imaging was

performed, using previously validated methods (Pereira et al., 1996) (refer to *Imaging Protocol* section below) to evaluate function and quantitative in vivo partition coefficient values in the tissue at risk (Region at Risk; RAR) and the remote tissue. The RAR tissue is defined as the region served by the stenotic artery and with blood flow <0.3 mL/min/g (measured by microspheres) during a complete transient occlusion (45 sec). Ex vivo tissue partition coefficient and viability were measured using $^{111}$In-DTPA and $^{201}$Tl, respectively, and compared to in vivo results, as previously reported (Pereira et al., 1996; Pereira et al., 2000; Thornhill et al., 2001).

## Animal Preparation and Surgery

All studies were in accordance with the University of Western Ontario Council on Animal Care guidelines. The results from 13 female dogs (three beagles, 10 mongrels) are reported in this study. Nine animals were studied for 3 weeks and four animals were studied for 10 weeks. Anesthesia was induced with Propofol 1% intravenously and then maintained using 2–2.5% isoflurane after endotracheal intubation. This was performed in preparation for surgery and all subsequent follow-up imaging sessions. During surgery, a left thoracotomy was performed to expose the heart and two small sections, each of approximately 0.8 cm in length, of the LAD were dissected free of the heart wall. The Doppler flow probe (proximal) and stenosing device (distal) were placed in these two regions, with the flow probe placed at least three vessel diameters proximal to the stenosing device. A femoral artery catheter was inserted for reference blood withdrawal during microsphere injections. Regional myocardial blood flow measurements were acquired at baseline, during the transient occlusion to determine the RAR, 15 minutes after stenosis formation, and just prior to sacrifice using four differently labeled, radioactive microspheres. Reference blood was withdrawn beginning one minute prior to the injection of either $^{141}$Ce-, $^{85}$Sr-, $^{46}$Sc-, or $^{95}$Nb-labeled microspheres (Perkin–Elmer, Boston, MA) directly into the left atrium, and continued for another 4 minutes at a rate of 1.94 mL/min. Coronary angiography was performed in eight dogs either following surgery or prior to sacrifice to validate the patency of the stenosed artery and confirm methodology (Fig. 1).

Two additional canines were acutely instrumented in the same fashion to assess perfusion reserve in our model of significant coronary artery stenosis. Adenosine stress was induced before and after stenosis formation using 0.14 mg/kg/min infusion maintained for 8 minutes. Radioactively labeled microspheres were injected at baseline, for RAR measurement, and 4 min into each adenosine infusion. $^{201}$Tl and $^{111}$In-DTPA were administered in the same manner as in the other animals to determine myocardial viability and distribution volume of Gd-DTPA. Animals were sacrificed immediately following the termination of the Gd-DTPA/$^{111}$In-DTPA 1 hr constant infusion, approximately 4 hours from the start of the experiment.

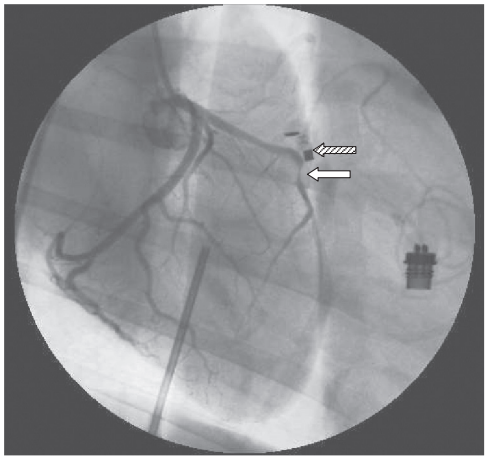

***Figure 1.*** X-ray angiogram in one animal after placement of Transonic flow probe and stenosing device. Hatched arrow indicates flow probe and white arrow indicates position of stenosing device around the LAD coronary artery. Stenosis degree in this animal was 76.2%; blood flow reduction in artery measured by flow probe was 71.7%. X-ray angiography was used to validate methodology and confirm creation of the stenosis.

## Imaging Protocol

Imaging was performed prior to surgery [Baseline (B), n=13], at 2–3 days (F1, n=13) and at 7 or 10 days (F2, n=13) following surgery, and weekly thereafter (F3–F10, no experiments at week 6) until the completion of the experiment at either 3 or 10 weeks. All imaging was performed on a Siemens Vision 1.5 T clinical system (Siemens, Erlangen, Germany), and the same imaging protocol was used for all imaging sessions. A schematic of this protocol is shown in Fig. 2. Animals were placed prone in a head coil, and the heart centered within the coil. Scout images were acquired, followed by precontrast saturation recovery turboFLASH (srTFL) images (TR/TE 2.4/1.2 ms, 8 mm slice thickness, 13° flip, FOV 300 mm) throughout the left ventricle. A 0.2 mmol/kg/min bolus of Gd-DTPA was injected at a rate of 46 mL/min, followed by a 1 hr constant infusion of 0.004 mmol/kg/min. Short axis, long axis, and four chamber cine images (TR/TE

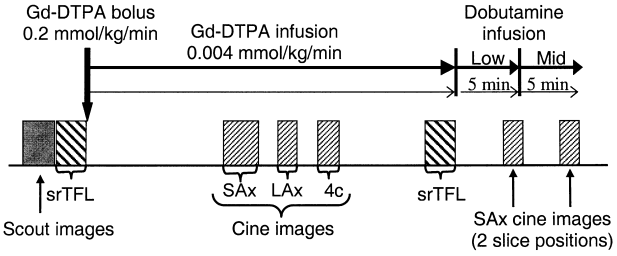


***Figure 2.*** Schematic timeline of MR imaging protocol for all follow-up imaging sessions. Dobutamine infusions—low-dose 5 μg/kg/min, mid-dose 10 μg/kg/min.

10/4.8 ms, 8 mm slice thickness, 30° flip, FOV 254–300 mm) were obtained to visualize contractile function for qualitative and quantitative analysis. The srTFL images were again acquired before the completion of the Gd-DTPA constant infusion for determination of in vivo partition coefficient (see *Image and Data Analysis* section below).

Low- and mid-dose dobutamine (5 μmol/kg/min and 10 μmol/kg/min, respectively) infusions were performed for 5 minutes each. Cine images were acquired at two slice positions in the last 2 minutes of each infusion to assess the inotropic reserve of myocardium subtended by the chronically stenosed coronary artery.

On the day of sacrifice, $^{201}$Tl (DuPont Canada, Markham, Ontario) was injected approximately 2.5 hr prior to sacrifice to assess tissue viability. The imaging protocol at sacrifice remained the same, but trace amounts of $^{111}$In-DTPA (Frosst Radiopharmaceuticals, Kirkland, Quebec, Canada) were added to the Gd-DTPA constant infusion and maintained until sacrifice to assess the distribution volume of DTPA chelates (i.e., measure partition coefficient) ex vivo. Just prior to sacrifice another measure of regional myocardial blood flow was obtained using microspheres.

Potassium chloride was injected to sacrifice the animal and the heart quickly excised and imaged using a high-resolution $T_1$-weighted 3D FLASH sequence

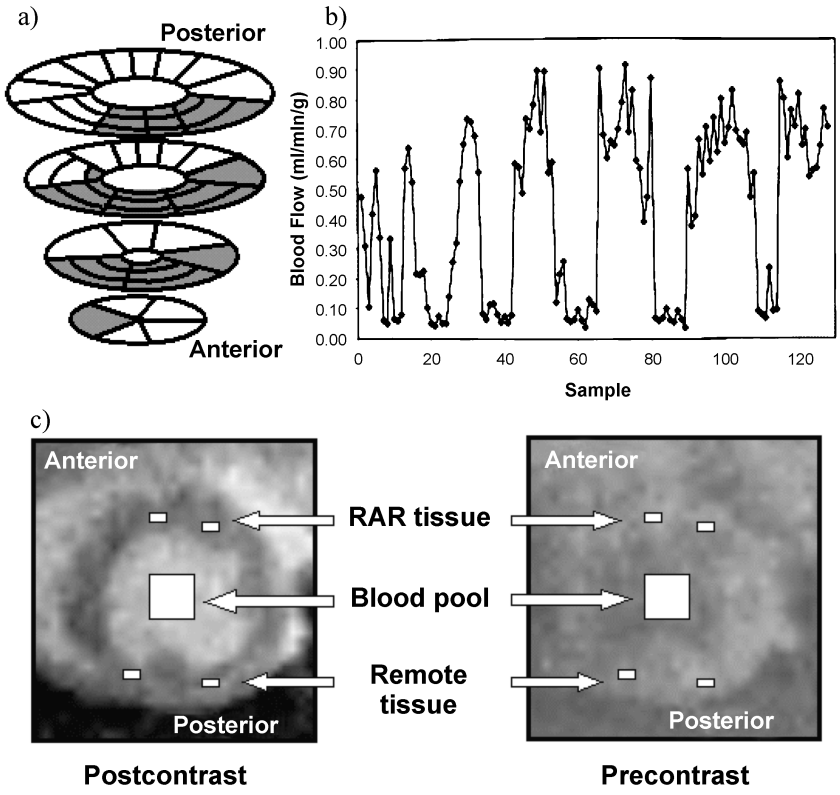


***Figure 3.*** a) Schematic of sectioning method used to determine blood flow, Tl uptake, and ex vivo partition coefficient in the tissue. Shaded areas represent tissue sections with blood flow <0.3 mL/min/g. b) Tissue blood flow of one dog during complete occlusion. Tissue samples with blood flow <0.3 mL/min/g were considered at risk for developing into reversible myocardial injury. c) Post- and precontrast srTFL images acquired to measure in vivo partition coefficient. Regions of Interest (ROIs) are drawn in the remote and RAR tissue, as well as the blood pool. Tissue regions at risk are determined by examining regional myocardial blood flow during a transient occlusion.



Marcel Dekker, Inc.
270 Madison Avenue, New York, New York 10016

(TR/TE 22/10 msec, 1 mm slice thickness, 40° flip, in-plane resolution 0.5 mm) to map the distribution of Gd-DTPA. The heart was then sliced into five to seven slices and visually inspected for signs of necrosis. The slices were then sectioned into 75–130 pieces weighing 0.2–1.2 g each. These tissue samples were counted for radioactivity to determine myocardial blood flow by microspheres, tissue viability by $^{201}$Tl uptake, and ex vivo partition coefficient of Gd-DTPA by $^{111}$In-DTPA (Pereira et al., 1996). Fig. 3a shows an example of how the heart is sectioned and Fig. 3b is an example of blood flow during the 45 sec occlusion that determines the RAR. This information is then used to assess the tissue viability, blood flow, and partition coefficient in the RAR and remote tissue.

### Image and Data Analysis

All data were analyzed after sacrifice, and the RAR tissue had been determined to ensure accurate analysis of RAR and remote tissue parameters. In vivo partition coefficient values were determined from the pre- and postcontrast srTFL images. Regions of Interest (ROIs) were drawn in the remote and RAR tissue (see Fig. 3c). The change in signal intensity (ΔSI) from post- to precontrast in both the tissue regions and the blood pool was determined using AnalyzeAVW (Robb, 1990) and in vivo partition coefficient was thus determined as (Pereira et al., 1999):

$$\lambda = \frac{\Delta SI_{tissue}}{\Delta SI_{blood}} \quad (1)$$

Quantitative wall motion was assessed by measuring left ventricular ejection fraction (LVEF) using Siemens-based software, ARGUS, which is a semi-quantitative segmentation program that draws contours around the blood pool of the end-diastolic and end-systolic images of each slice and calculates LVEF as:

$$\text{LVEF} = \frac{\text{EDV} - \text{ESV}}{\text{EDV}} \times 100 \quad (2)$$

Qualitative wall motion analysis was performed on all cine MR images throughout the left ventricle at every time-point in each animal, including after low- and mid-dose dobutamine infusions. Each short axis cine at each slice position was assessed for wall motion in six different regions: septal, anteroseptal, anterolateral, lateral, inferolateral, and inferoseptal. An experienced cardiologist (GW), blind to the cardiac states of each wall motion study, scored each of these regions on a scale from 0–6. The scoring was as follows: 0—hyperkinetic, 1—normal, 2—mildly hypokinetic, 3—moderately hypokinetic, 4—severely hypokinetic, 5—akinetic, and 6—dyskinetic.

Average blood flow, ex vivo partition coefficient, and normalized Tl uptake values were calculated in both the RAR tissue and remote tissue. In vivo partition coefficient values were calculated by placing ROIs (method described above) in the regions that corresponded to tissue sections with reduced blood flow during the 45 sec occlusion, and therefore at risk of forming reversible myocardial injury.

### Perfusion Reserve Determination

Perfusion reserve during adenosine stress was determined in two separate animal experiments as noted above in *Animal Preparation and Surgery*. Perfusion reserve was calculated as average regional myocardial blood flow in the RAR and remote tissue during adenosine stress normalized by regional myocardial blood flow at rest in the same tissue regions.

### Statistical Analysis

All result values are expressed as mean value plus or minus standard error of the mean (SEM). Analysis of Variance (ANOVA) was performed on the blood flow, in vivo and ex vivo partition coefficient, normalized Tl uptake, and quantitative functional data to determine the relationship between the RAR and remote tissue regions of these parameters. If the ANOVA revealed significance, further investigation was performed using Tukey posthoc analysis. Levene's statistic was computed to determine whether homogeneity of variance was present or not. If not, inhomogeneous data sets were square-root transformed and analyzed in the same manner as listed above. If homogeneity of variance was still not present, nonparametric statistical analysis was performed and compared to results obtained using parametric tests. Repeated measures analysis was performed on the qualitative wall motion data to determine if a relationship existed between the RAR and remote tissue regions at the various time-points studied. Nonparametric analysis was performed to confirm parametric results since the wall motion scoring was a subjective analysis. An alpha value of $P<0.05$ was considered significant.

## RESULTS

The acute functional effects of the coronary stenoses averaged 72.4±1.6% (n=9) below baseline values, determined by the flow change through the LAD using the flow probe. Luminal diameter reduction using x-ray angiography revealed an approximate stenosis degree of 75–80% (all dogs). Regional

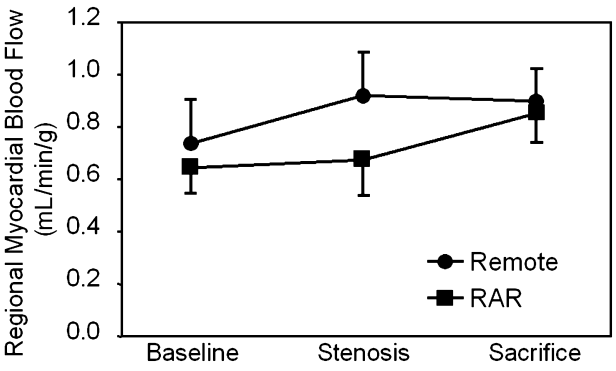


***Figure 4.*** Regional myocardial blood flow in the RAR tissue (■) and in the remote tissue (●) at baseline, 15 min after stenosis formation, and just prior to sacrifice. Error bars represent SEM. No significant differences were noted either between the tissue regions or over the three different measurements.

myocardial blood flow results, determined by radioactive microspheres, are shown in Fig. 4. All blood flow measurements were taken at rest under general anesthetic. Baseline blood flow was 0.64 mL/min/g in the RAR and 0.74 mL/min/g in the remote tissue. Blood flow in both the RAR and remote tissue was insignificantly increased (0.67 mL/min/g and 0.92 mL/min/g, respectively; P=NS) 15 min following the stenosis formation compared to baseline. At sacrifice, blood flow was again insignificantly increased in both the RAR (0.85 mL/min/g; P=NS) and remote tissue (0.90 mL/min/g; P=NS), despite maintained stenosis formation. Although blood flow tended to be higher in the remote tissue compared to the RAR tissue at all time-points measured, there was no significant difference in the flow to these regions at any time.

The normalized Tl uptake results from 11 animals and ex vivo partition coefficient results from all 13 animals are shown in Table 1, as well as the mean and SEM values. In two animals, $^{201}$Tl was not available at the time of sacrifice. A minor 3% significant reduction was noted in the normalized Tl uptake values in the RAR vs. remote tissue ($P<0.05$). However, the Tl uptake values were within the range of normal tissue in both the RAR and remote tissue. No significant difference in ex vivo λ was noted between the two tissue regions.

All in vivo partition coefficient results for the duration of the experiment in all dogs are shown in Fig. 5. Average values ranged between 0.31–0.42 mL/g in remote tissue and 0.32–0.45 mL/g in RAR tissue. The partition coefficient of the remote tissue was significantly lower than that of the RAR tissue at day 14 (0.34 mL/g vs. 0.39 mL/g; $P<0.05$). No other significant

***Table 1.*** Normalized Tl uptake and ex vivo λ results in both the remote and RAR tissue in all 13 dogs.

| | TI Uptake* | | Ex vivo λ | |
|---|---|---|---|---|
| DOG | REM | RAR | REM | RAR |
| 1 | 0.99 | 0.95 | 0.21 | 0.18 |
| 2 | 0.97 | 0.89 | 0.45 | 0.31 |
| 3 | 0.98 | 0.90 | 0.33 | 0.33 |
| 4 | 0.96 | 0.95 | 0.34 | 0.42 |
| 5 | 0.96 | 0.94 | 0.31 | 0.32 |
| 6 | 0.94 | 0.94 | 0.33 | 0.49 |
| 7 | 0.94 | 0.92 | 0.34 | 0.32 |
| 8 | 0.94 | 0.95 | 0.49 | 0.38 |
| 9 | 0.95 | 0.92 | 0.28 | 0.28 |
| 10 | N/A | N/A | 0.33 | 0.34 |
| 11 | N/A | N/A | 0.29 | 0.29 |
| 12 | 0.95 | 0.96 | 0.39 | 0.39 |
| 13 | 0.97 | 0.91 | 0.34 | 0.34 |
| AVG | 0.96 | 0.93 | 0.34 | 0.34 |
| SEM | 0.005 | 0.007 | 0.020 | 0.021 |

Also shown are the average values and SEM. A significant (*) difference was noted between the remote and RAR Tl uptake. Tl uptake and λ were within the range of normal tissue in both the RAR and remote tissue, and all tissue regions were considered viable based on the Tl uptake values.

differences were found either within or between the remote and RAR tissue groups. All values were below 0.7 mL/g, the upper limit for normal λ. Therefore, all λ values were within the range of normal tissue. Additionally, no signs of infarction were noted during the visual inspection during sectioning of the heart.

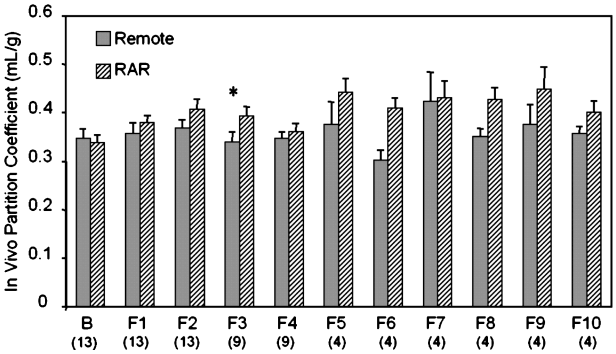


***Figure 5.*** In vivo partition coefficient results in remote tissue and tissue at risk prior to surgery (B) and at the follow-ups after surgery (F1–F10). (Numbers) indicate ''n'' at each imaging session. Error bars indicate the standard error of the mean. Significance (*) between the RAR and remote tissue was noted at F3 (Day 14). No significant differences within the tissue groups were found.

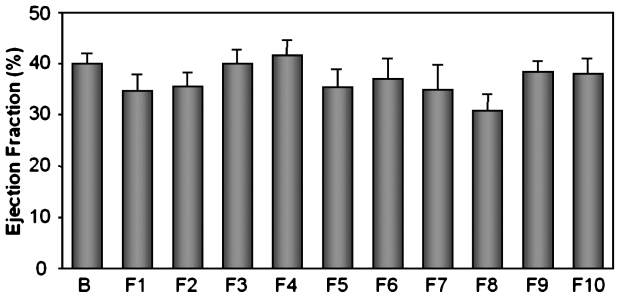


*Figure 6.* Left ventricular ejection fraction (%) results in all dogs at rest at Baseline (B) and Follow-ups 1–10 (F1–F10). Error bars represent SEM. LVEF did not change over either the 3-week or 10-week protocols.

Left ventricular ejection fraction (LVEF) results from all dogs are shown in Fig. 6. Average ejection fraction values ranged from 30.8% to 41.7%. No significant differences were noted at any time-point. Normalization of global ejection fraction results to heart rate revealed similar results as without normalization, although there did appear to be a tendency for normalized ejection fraction to be slightly reduced up to one week following stenosis formation.

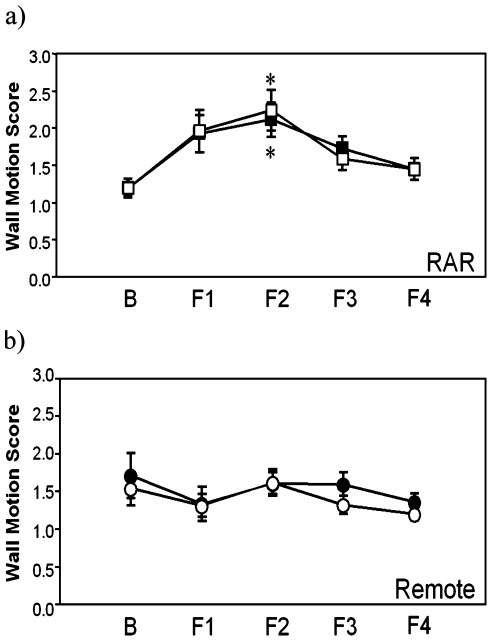


*Figure 7.* Wall motion scores at rest throughout the experiment in the (a) RAR and (b) remote tissue. a) RAR tissue; significant decrease in wall thickening score at Day 10 compared to baseline. b) Remote tissue; no significant change in wall thickening score. Key: RAR tissue: ■, mid-apical slice, □, mid-basal slice; Remote tissue: ●, mid-apical slice ○, mid-basal slice. * indicates significance at Day 10 (F2) in two different slice positions ($P<0.05$).

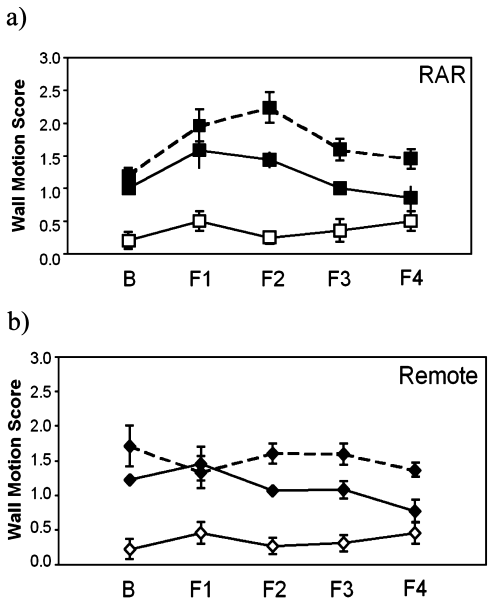


*Figure 8.* Wall motion scores during dobutamine stimulation in one slice position in the (a) RAR, and (b) remote tissue regions. Dashed line, At rest; Solid symbol, 5 min low-dose dobutamine; Open symbol, 5 min mid-dose dobutamine.

Qualitative regional wall motion results in all 13 animals at rest and during stress up to Follow-up 4 (F4) (21 days) are shown in Figs. 7 and 8, respectively. Wall motion in the RAR in the four animals studied up to 10 weeks was not different from the wall motion seen at Follow-up 4. The RAR tissue results from two slice positions are shown in Fig. 7a, and the remote tissue results from the same two slice positions are shown in Fig. 7b. Wall motion in the RAR tissue was significantly decreased at F2 (10 days), with higher wall motion score following stenosis formation ($P<0.05$), but had returned to baseline values by either 3 ($n=9$) or 10 ($n=4$) weeks. In the remote tissue, significant changes in regional function were not observed. Wall motion in all remote regions was similar and had a wall thickening score of approximately 1 (normal wall motion). Of the 13 animals studied, 10 (76%) demonstrated an evident regional reduction in wall motion score at F2 that returned to baseline by F4.

Wall motion results during dobutamine stress are shown in Fig. 8 from one slice position in the RAR (a), and remote (b) tissue regions. Image quality from the most apical slice was poor due to increased motion artefact and hence could not be reliably analyzed. Statistical analysis was performed only on those animals

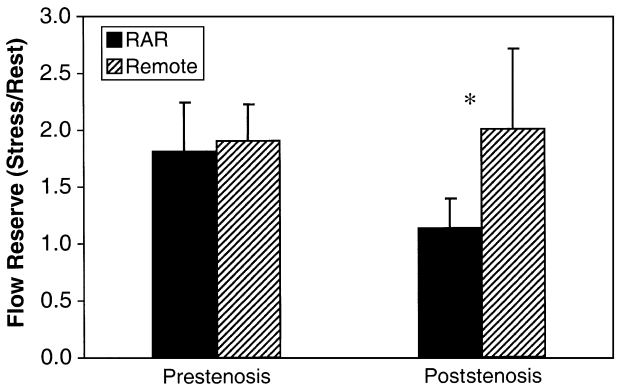


***Figure 9.*** Perfusion reserve in two additional dogs before and 30 min after stenosis formation in both the RAR and remote tissue is calculated as blood flow during stress divided by blood flow at rest. Infusing 0.14 mg/kg/min adenosine for 8 minutes induced stress, and blood flow was measured by injecting radioactively labeled microspheres 4 min into infusion. Perfusion reserve was significantly (*; $P<0.001$) attenuated in the tissue distal to the stenosis (RAR tissue) compared to remote tissue following stenosis formation.

with complete dobutamine image sets. No significant differences between time and dobutamine dose were noted (7/13 dogs, slice 1 and 4/13 dogs, slice 2). In both the RAR and remote tissue regions, low-dose and mid-dose dobutamine increased function at each time-point. As expected, low-dose dobutamine increased function to a lesser degree than mid-dose dobutamine.

Perfusion reserve results are shown in Fig. 9. Perfusion reserve was attenuated in the RAR tissue after stenosis formation compared to the same tissue region prior to stenosis (1.20 mL/min/g vs. 1.89 mL/min/g; $P<0.001$). Perfusion reserve was comparable in the remote tissue after stenosis formation compared to prior to stenosis (1.99 vs. 1.90 mL/min/g; P=NS).

## DISCUSSION

Since $^{201}$Tl uptake and both the in vivo and ex vivo partition coefficient values were within the normal range, with no evidence of myocardial necrosis upon visual inspection, increases in partition coefficient are demonstrated, in this study, to be specific for the detection of infarcted myocardium. Our group (Thornhill et al., 2001) and others (Kim et al., 2000) have previously shown this to be a sensitive method for detecting myocardial necrosis.

Despite a significant stenosis maintained throughout both the 3-week and 10-week experiments, regional myocardial blood flow at rest, measured with microspheres, was not reduced, in contrast to previous reports using a similar model in swine (Liedtke et al., 1995). However, when we attempted to increase the stenosis degree to greater than 75–80%, in the quest to reduce resting blood flow, infarction resulted. In fact, resting blood flow in this study was actually slightly increased (although insignificantly) in both the tissue at risk and remote tissue following stenosis and at sacrifice. Kudej et al. (1998) also noted a gradual increase in coronary artery blood flow in pigs after formation of stenosis with a hydraulic occluder and readjusted the occluder to match the desired blood flow reduction originally achieved, which resulted in myocardial infarction. The increase in blood flow observed in our current experiments could either be a transient compensatory mechanism (acutely) or an increase in collateral recruitment (acutely) or development (chronically). Our experiments have shown that a significant but noncritical (flow limiting) coronary artery stenosis in a single vessel does not lead to a progressive reduction in resting blood flow or contractile function, and would not appear to produce the clinical phenomenon of hibernating myocardium in this canine model.

Some groups (Gerber et al., 1996; Vanoverschelde et al., 1993) have reported that hibernating myocardium is a by-product of repeated intermittent episodes of stress or demand-provoked ischemia associated with stunning, with normal resting flow initially, rather than being caused by a sustained decrease in perfusion. Each episode of stunning, with transient left ventricular dysfunction, ultimately culminates in persistent chronic dysfunction or hibernating myocardium. In this study, however, regional dysfunction only occurred at 10 days and did not persist throughout the experiment, despite repeated sessions of pharmacological stress by dobutamine and the fact that the animals' daily activity, including run exercise, was not restricted. The acute studies demonstrated that perfusion reserve was reduced at the time of surgery, but we could not obtain similar information during the course of the 3- or 10-week studies. It may therefore be possible that perfusion reserve was only restricted at the time of surgery and normalized over time, and may explain why hibernating myocardium was not produced. Further experiments will monitor perfusion reserve over the entire 3-week protocol, using the same model. Of importance to note, however, is that in the 10-week experiments, x-ray angiography was performed both early and late, and no significant change in stenosis degree was noted over that time frame.

Canty and Fallavollita (1999, 2001) stress the importance of studying models of noncritical but flow

reserve limiting stenosis, creating hibernating myocardium, for longer periods of time, possibly up to 3 months, before tissue with reduced blood flow and function will develop. In our experiments, with a maintained significant coronary stenosis, similar in degree to the percentage stenosis reported by these investigators, neither resting myocardial blood flow nor contractile function was reduced compared to baseline after 10 weeks. We conclude that chronic hibernating myocardium does not develop within up to ten weeks of chronic significant coronary artery stenosis in this model. At this point, we are unsure why dysfunction developed only at 10 days and did not persist to 3 or 10 weeks. The 45sec, transient occlusion was not sufficient to cause a reduction in wall motion. Additionally, this transient occlusion was performed at the conclusion of the experiment in the 10-week experiments, rather than at the beginning of experiments as in the 3-week protocol, and wall motion reduction was still noted. Possibly the manipulation of the coronary artery during surgery might explain why the reduction in function occurs, although not on a delayed basis. However, this is only speculative and does not explain the reduction in wall motion at only one time-point.

The quest for a sensitive and specific measure of myocardial viability is extremely important (Thornhill et al., 2003), since restoration of blood flow could restore function to dysfunctional regions. The sensitivity of contrast-enhanced MRI is well-known; however, the specificity has been challenged by delayed enhancement experiments performed in rats that argue that infarct size is overestimated due to a transient increase in partition coefficient in reversibly damaged tissue surrounding the infarct zone (Oshinski et al., 2001; Saeed et al., 2001). Our use of a constant infusion technique, as opposed to delayed enhancement, eliminates any altered washout effects, since this technique eliminates the effect of flow on enhancement (Tong et al., 1993). The results found in this study indicate that partition coefficient is not increased in reversibly damaged myocardium, as manifest by the transient reduction in contractility, caused by a significant coronary artery stenosis, which further implies that MRI is a specific indicator of myocardial viability. However, further studies of other types of reversible damage, especially hibernating myocardium, will have to be done to confirm the specificity of this method.

This study reports that in the case of chronic coronary artery stenosis, partition coefficient values remain within the range of normal tissue. Although hibernating myocardium was not created, as per the original goal of this project, the results obtained give additional insight into the mechanisms leading/not leading to hibernating myocardium and, in fact, do not support the notion that it occurs secondary to repetitive stunning. Also, given that $^{201}$Tl uptake was normal in both the tissue at risk and the remote tissue, the experiments provide further evidence that the measurement of the partition coefficient of Gd-DTPA using MRI is both a sensitive and specific indicator of tissue viability.

## ABBREVIATIONS

| | |
|---|---|
| srTFL | saturation recovery turboFLASH |
| SAx | short axis |
| LAx | long axis |
| 4c | 4 chamber |

## ACKNOWLEDGMENTS

The authors would like to thank Jenny Gibbons and Lela Noonan for animal and experiment assistance; Dick J. Drost for technical assistance using the Siemens MR unit; Berlex Canada for providing Gd-DTPA (Magnevist™ formulation); Yves Bureau for statistical analysis assistance; and the Canadian Institutes for Health Research, the Ontario government, and the Natural Sciences and Engineering Research Council of Canada for financial support.

## REFERENCES

Canty, J. M. Jr., Fallavollita, J. A. (1999). Resting myocardial flow in hibernating myocardium: validating animal models of human pathophysiology. *Am J. Physiol.* 277(1 Pt 2):H417–H422. Review.

Canty, J. M., Fallavollita, J. A. (2001). Lessons from experimental models of hibernating myocardium. *Coron. Artery Dis.* 12:371–380.

Gerber, B. L., Vanoverschelde, J.-L., Bol, A., Michel, C., Labar, D., Wijns, W., Melin, J. A. (1996). Myocardial blood flow, glucose uptake, and recruitment of inotropic reserve in chronic left ventricular ischemic dysfunction. Implications for the pathophysiology of chronic myocardial hibernation. *Circulation* 94:651–659.

Kim, R. J., Wu, E., Rafael, A., Chen, E.-L., Parker, M. A., Simonetti, O., Klocke, F. J., Bonow, R. O., Judd, R. M. (2000). The use of contrast-enhanced magnetic resonance imaging to identify reversible

myocardial dysfunction. *N. Engl. J. Med.* 343: 144–153.

Kudej, R. K., Ghaleh, B., Sato, N., Shen, Y.-T., Bishop, S. P., Vatner, S. F. (1998). Ineffective perfusion-contraction matching in conscious, chronically instrumented pigs with an extended period of coronary stenosis. *Circ. Res.* 82:1199–1205.

Liedtke, A. J., Renstrom, B., Nellis, S., Hall, J. L., Stanley, W. C. (1995). Mechanical and metabolic function in pig hearts after 4 days of chronic coronary stenosis. *JACC* 26(3):815–825.

Oshinski, J. N., Yang, Z., Jones, J. R., Mata, J. F., French, B. A. (2001). Imaging time after Gd-DTPA injection is significant in using delayed enhancement to determine infarct size accurately with magnetic resonance imaging. *Circulation* 104:2838–2842.

Pereira, R. S., Prato, F. S., Wisenberg, G., Sykes, J. (1996). The determination of myocardial viability using Gd-DTPA in a canine model of acute myocardial ischemia and reperfusion. *Magn. Reson. Med.* 36:684–693.

Pereira, R. S., Prato, F. S., Sykes, J., Wisenberg, G. (1999). Assessment of myocardial viability using MRI during constant infusion of Gd-DTPA: further studies at early and later periods of reperfusion. *Magn. Reson. Med.* 42:60–68.

Pereira, R. S., Prato, F. S., Lekx, K. S., Sykes, J., Wisenberg, G. (2000). Contrast-enhanced MRI for the assessment of myocardial viability after permanent coronary artery occlusion. *Magn. Reson. Med.* 44:309–316.

Robb, R. A. (1990). A software system for interactive and quantitative analysis of biomedical images. In: Høhne, K. H., Fuchs, H., Pizer, S. M., eds. *3D Imaging in Medicine, NATO ASI Series*. Berlin: Springer-Verlag, pp. 333–361.

Received July 9, 2002
Accepted July 13, 2003

Saeed, M., Lund, G., Wendland, M. F., Bremerich, J., Weinmann, H.-J., Higgins, C. B. (2001). Magnetic resonance characterization of the peri-infarction zone of reperfused myocardial infarction with necrosis-specific and extracellular nonspecific contrast media. *Circulation* 103: 871–876.

Schwitter, J., Saeed, M., Wendland, M. F., Derugin, N., Canet, E., Brasch, R. C., Higgins, C. B. (1997). Influence of severity of myocardial injury on distribution of macromolecules: extravascular versus intravascular gadolinium-based magnetic resonance contrast agents. *JACC* 30(4):1086–1094.

Thornhill, R. E., Prato, F. S., Pereira, R. S., Wisenberg, G., Sykes, J. (2001). Examining a canine model of stunned myocardium using Gd-DTPA-enhanced MRI. *Magn. Reson. Med.* 45(5):864–871.

Thornhill, R. E., Prato, F. S., Wisenberg, G. (2003). The assessment of myocardial viability: a review of current diagnostic imaging approaches. *JCMR* 4(3):381–410.

Tong, C. Y., Prato, F. S., Wisenberg, G., Lee, T. Y., Carroll, E., Sandler, D., Wills, J. (1993). Techniques for the measurement of the local myocardial extraction efficiency for inert diffusible contrast agents such as gadopentate dimeglumine. *Magn. Reson. Med.* 30:332–336.

Vanoverschelde, J.-L., Wijns, W., Depré, C., Essamri, B., Heyndrickx, G. R., Borgers, M., Bol, A., Melin, J. A. (1993). Mechanisms of chronic regional post-ischemic dysfunction in humans: new insights from the study of noninfarcted collateral-dependent myocardium. *Circulation* 87:1513–1523.

Wijns, W., Vatner, S. F., Camici, P. G. (1998). Mechanisms of disease: hibernating myocardium. *New Engl. J. Med.* 339(3):173–181.



MARCEL DEKKER, INC.
270 Madison Avenue, New York, New York 10016